Available online at www.sciencedirect.com

ScienceDirect

Acta Materialia 59 (2011) 3937–3945

Acta MATERIALIA

www.elsevier.com/locate/actamat

Residual plastic strain recovery driven by grain boundary diffusion in nanocrystalline thin films

Xiaoding Wei *, Jeffrey W. Kysar

Department of Mechanical Engineering, Columbia University, New York, NY 10027, USA

Received 17 November 2010; received in revised form 24 February 2011; accepted 8 March 2011
Available online 1 April 2011

Abstract

Residual strain in metals is typically considered to be irreversible. However, residual strain in nanocrystalline materials can be recovered over a period of time via diffusive mechanisms. In this study, free-standing copper films of submicron thickness with an average grain size of about 40 nm are mechanically loaded via a plane-strain bulge test, and residual strain recovery at room temperature is characterized after unloading. The specimens recover their residual strain in a period of time that can range from a few days to more than 1 month depending upon the surface conditions and heterogeneous residual strain distributions in multiple cycles of recoveries. A constant tensile stress of about 25 MPa is reached after each recovery finishes. Two characteristic strain rates occur during residual strain recovery, a transient strain recovery rate of the order of 10^{-7} s^{-1} and a steady-state strain recovery rate of the order of 10^{-9} s^{-1}. A model of the plastic strain recovery is presented which demonstrates the plausibility that grain boundary diffusion driven by chemical potential gradients due to residual stresses and the presence of voids can rationalize the transient and steady-state plastic strain recovery rates, respectively.
Published by Elsevier Ltd. on behalf of Acta Materialia Inc.

Keywords: Nanocrystalline; Plasticity; Grain boundary diffusion; Plastic strain recovery

1. Introduction

Nanocrystalline metals [1–4] are characterized by a grain size that is of the order of a few tens of nanometers. They are of interest due to their significantly higher strength relative to metals with a grain size of the order of micrometers. This is especially true for nanocrystalline metals in the form of thin films because very few other standard strengthening strategies, e.g. alloying, exist for thin films [5]. A plethora of different deformation mechanisms can operate in metals under a broad range of conditions, time scales and length scales, including diffusion, dislocation creation and motion, twinning, fracture, and grain boundary sliding [6–7]. Often, nanocrystalline (NC) metals are stronger than their coarse-grained counterparts due to the relative paucity of dislocation-mediated plasticity within the nanometer length-scale grains [1,2].

Recent experiments by Rajagopalan et al. [3] showed that nanocrystalline thin films of Al and Au were able to recover residual plastic strain. In those experiments, face-centered cubic NC free-standing specimens were deformed in tension within a microelectromechanical (MEMS) device past the yield point to induce plastic deformation; the resulting plastic strain is typically considered to be permanent. Remarkably, Rajagopalan et al. report that a portion of the plastic strain in their specimens was recovered over the course of several minutes to several hours.

In this paper, we report experimental observations of plastic strain recovery in free-standing thin films of face-centered cubic NC metals. The experiments are performed using a thin film bulge test to impart a load to the NC metal films. After inducing a significant degree of plastic deformation (up to 0.5% total engineering strain), the load

* Corresponding author. Present address: Northwestern University, 2145 Sheridan Road, Evanston, IL 60208-3111, USA. Tel.: +1 646 463 3239; fax: +1 847 491 8539.
E-mail address: x-wei@northwestern.edu (X. Wei).

1359-6454/$36.00 Published by Elsevier Ltd. on behalf of Acta Materialia Inc.
doi:10.1016/j.actamat.2011.03.019

is removed prior to failure of the film. Since the free-standing film has lengthened, it develops a buckling pattern visible to the naked eye upon removal of the load. With time (from a few hours to a few weeks, depending upon conditions), the film shortens and eventually recovers a flat profile. We employ a scanning laser confocal microscope to measure the profile of the buckled free-standing film, from which it is straightforward to determine the length of the buckled film. By continuously monitoring the length of the buckled film, we measure the rate at which the plastic strain recovers, and find both a characteristic transient rate of plastic strain recovery as well as a steady-state rate of plastic strain recovery. Indeed, the measurements show that the nanocrystalline film not only recovers its originally flat profile, but also develops a residual tensile (!) stress under the influence of no external tractions.

Many potential deformation mechanisms may be activated in a load-recovery cycle, including dislocation-mediated plastic deformation either from sources within a grain or from grain boundaries [8]; twinning (at least in some materials) at the very high stresses seen during the loading [6,9]; grain boundary sliding [10]; and diffusive mechanisms [11]. In this paper, we postulate that the observed plastic strain recovery occurs as a consequence, predominantly, of grain boundary diffusion. To that end, we develop a simple model that accounts for diffusive flow over distances shorter than the grain size, as well as for diffusive flow over distances larger than a typical grain size. The simple model is able to capture both the transient and the steady-state plastic strain recovery rates, which demonstrates the plausibility of the assumption that the plastic strain recovery is driven predominantly by grain boundary diffusion.

This paper is organized in the following way. Section 2 describes the fabrication of the specimens, the thin film bulge test, as well as the plastic strain recovery measurements. Section 3 discusses the results of the experiments with regard to the dominant deformation mechanisms active during a load-recovery cycle. The simple model of grain boundary diffusion-driven plastic strain recovery is introduced in Section 4. Then in Section 5 we compare the results of the model to the experiments. Finally, we draw conclusions in Section 6.

2. Experiments

The specimens are thin films of NC Cu deposited by thermal vapor deposition onto single-crystal Si wafers that have a thin Si_3N_4 layer. Standard processes are used to etch away the Si and Si_3N_4 layer to obtain a free-standing metal film. The films themselves have thicknesses that range from 200 to about 600 nm, and the average grain size is between 35 and 40 nm, as measured using a scanning electron microscope (Hitachi 4700) and X-ray diffraction (Inel XRD 3000). The dimensions of the free-standing film are 1 mm × 10 mm. Thus, the thickness to width ratio is less than 10^{-3}, and the film can therefore be treated as a membrane rather than as a plate. Full details of the fabrication of the films can be found in Ref. [5].

The mechanical properties of the films are characterized with a plane-strain bulge test setup [5] using nitrogen gas to apply the pressure as illustrated in Fig. 1. The strain rate of loading can be varied by four orders of magnitude from about 10^{-8} to about $10^{-4}\,s^{-1}$. During loading, the film adopts a circular profile due to the pressure (since the film can be treated as a membrane), and the radius of curvature of the deformed film is measured via scanning laser confocal profilometer (Keyence, Inc.; with out-of-plane resolution of 10 nm and in-plane spatial resolution of 2 μm). The nominal stress and engineering strain in the film are:

$$\sigma = \frac{PR}{h}, \tag{1}$$

$$\varepsilon = \frac{R}{a}\arcsin\left(\frac{a}{R}\right) - 1, \tag{2}$$

where P is applied gauge pressure, h is the film thickness, R is the radius of the deformed film and a is the half-width of the film.

A feedback control system is employed for these experiments to obtain a strain rate of $10^{-6}\,s^{-1}$ upon loading. If the pressure on the film is removed prior to film failure, the film—having lengthened—buckles elastically into a shape (cf. Fig. 2a) that minimizes its potential energy. The laser scanning profilometer measures the out-of-plane profile of the film in its buckled state. The length of the film is then determined by elementary numerical differentiation and integration of the measured profile.

One such profile of a buckled film as measured with the confocal laser profilometer immediately after removal of the pressure is shown in Fig. 2b. It is important to note that the film is not under the influence of any externally applied traction in its buckled state after unloading, other than the negligible stress due to film bending due to edge constraints. Thus it is remarkable that the film begins to shorten immediately after unloading. In the specimens studied herein, the plastic strain recovery proceeds until all the plastic strain in the film recovers and the film is again flat, as if in its original state, as shown in Fig. 2a.

When the film is again loaded in the bulge test apparatus, the stress–strain response of the recovered material indicates there to be a residual tensile stress in the film. Thus, not only did the NC metal recover its plastic strain,

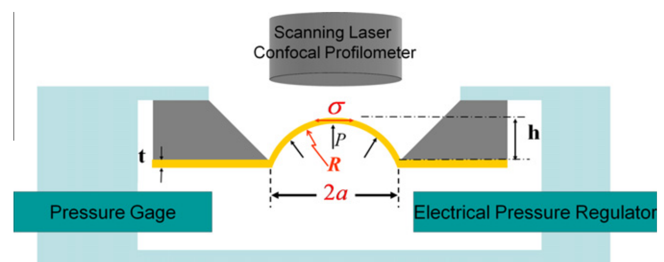

Fig. 1. Schematic of plane-strain bulge test setup. A laser scanning confocal profilometer measures the radius of curvature of deformed shape of film; an electrical pressure regulator controls the pressure applied to the film and a pressure gage measures the pressure inside the chamber.

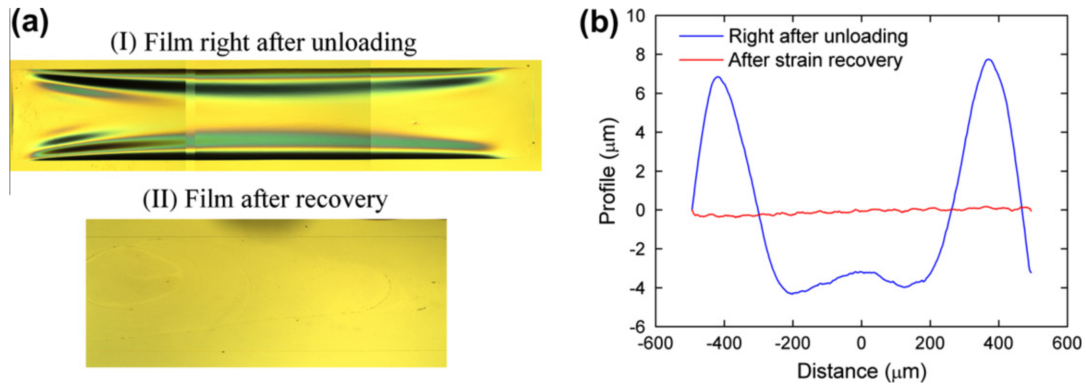

Fig. 2. (a) Optical images of film (~1 mm wide) before (I) and after (II) strain recovery. (b) Profiles of same film across its width immediately after pressure was removed and after residual recovery finished.

but the film deforms under no external loading until it has introduced itself into a state of residual tension. This process can be repeated several times on a film before it fails due to rupture or ripping at high pressure. The main difference in subsequent load–unload cycles is that the plastic strain recovery rate is somewhat slower, but the magnitude of the final tensile stress in the film is the same after the subsequent cycles as after the first cycle.

An example of the history of one NC Cu thin film with a thickness of 190 nm is shown in Fig. 3a. The film was loaded three times and each time the plastic strain in the film was recovered over a period of time ranging from 2 days to about a month. The films achieved a tensile stress of about 25 MPa after strain recovery, as seen in the stress–strain response from the second and third tests. Furthermore, after offsetting the curves to account for the initial strains from the three tests as shown in Fig. 3b, it is apparent that the film exhibits slight, but evident, strain hardening after each recovery, as opposed to the experiments in Ref. [3] which exhibited negligible strain hardening.

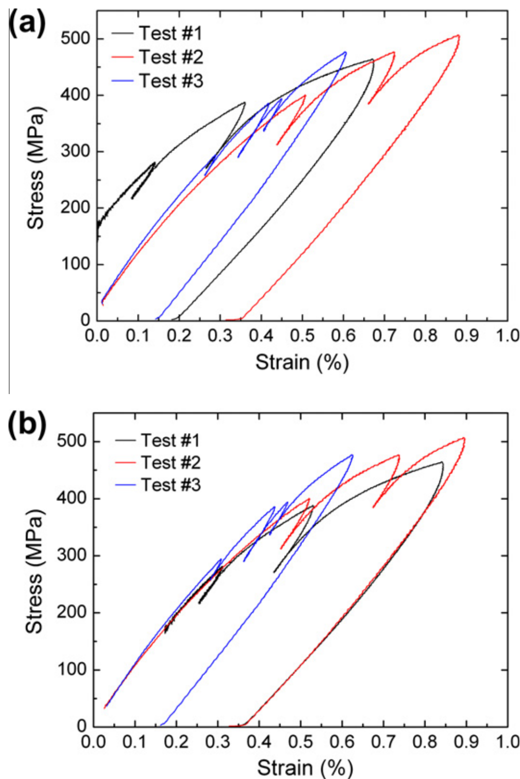

Fig. 3. (a) Stress–strain curves of three tests for same nanocrystalline Cu film. (b) Offset stress–strain curves for the same three tests.

Fig. 4 shows the recovered plastic strain as a function of time for the three load cycles; the time on the abscissa of Fig. 4 initiates at the moment the pressure is removed. The strain recovery process for each load cycle has a transient stage during which the plastic strain recovery rate is of the order of 10^{-7} s^{-1}, followed by a transition to what we term a steady-state plastic strain recovery rate of the order of 10^{-9} s^{-1}. The steady-state plastic strain recovery rates become progressively smaller, but still within the same order of magnitude, as the number of load cycles increases. In fact, the first plastic strain recovery cycle finished in about 2 days, but the second and third recoveries took up to a month, and hence were recorded only in the first few tens of hours until the steady-state recovery conditions were achieved. The specimen was maintained at ambient temperature (~300 K) throughout the entire experiment.

3. Interpretation of experiments

During the loading phase, dislocation-mediated plastic deformation may be activated within the grains, but the

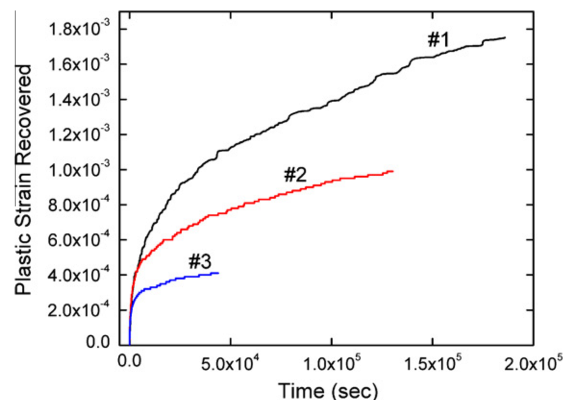

Fig. 4. Plastic strain recovery vs. time for the three recovery cycles.

grain size is typically too small for volume dislocation sources to exist, so dislocation sources are thought to be predominantly from grain boundaries [1,7,12–14]. Evidence for this exists in the broadening of X-ray diffraction peaks during loading of NC metals [8]. After the loading is removed from a NC metal, the X-ray diffraction experiments [8] show that the peak broadening is reversible, which indicates that the grain boundaries act as dislocation sinks as well as likely dislocation sources. Therefore, the dislocations move to the grain boundaries after the loading is removed. Hence, dislocation-mediated plastic deformation may play some role in the plastic strain recovery process.

However the volume fraction of grain boundaries in a NC material ranges from 27% to 7% for grain sizes, respectively, of 10 and 40 nm [14], assuming a grain boundary thickness of 0.5 nm. In addition, grain boundaries are often relatively wide regions of atomic disorder that extend two or three lattice spacings [15]. Thus, grain boundaries are typically weaker than grains, so much of the deformation may also proceed by grain boundary sliding during loading, at least at sufficiently small strain rates for which grain boundary diffusion can play an important role.

Returning now to the experiments on plastic strain recovery discussed herein. Because no external tractions act on the NC thin film during plastic strain recovery, the dominant mechanism during plastic strain recovery must be driven solely by internal driving forces such as residual stresses and other gradients in chemical potential. The residual stress in the grains may drive existing dislocations in the grains to the grain boundaries, but it is unlikely to nucleate new dislocations from grain boundary sources. As a consequence, dislocation-mediated plastic deformation may be responsible for a portion—but not all—of the plastic strain recovery [8]. The most probable mechanism during plastic strain recovery, then, is due to diffusion driven by gradients in chemical potential. Given the very high volume fraction of grain boundaries in a NC material as compared to a microcrystalline counterpart, the diffusion paths are likely to be along grain boundaries. In addition, recent atomistic modeling of NC Al [16] with a similar average grain size also suggested grain boundary and dislocation-mediated mechanisms coexist in the plastic strain recovery phenomena.

It is instructive to calculate the typical diffusion distances expected along grain boundaries for the temperatures and times encountered during plastic strain recovery. The mean diffusion distance of atoms [17] along a one-dimensional grain boundary during time t is $l_d = \sqrt{2D_b t}$, where the grain-boundary diffusivity, D_b, can be expressed as $\delta_b D_b = \delta_b D_{b0} \exp(-Q/RT)$, where R is the universal gas constant, T is the absolute temperature, with the pre-factor $\delta_b D_{b0} = 1.16 \times 10^{-15}\ \mathrm{m^3\,s^{-1}}$ and an activation energy $Q = 84.75 \times 10^3\ \mathrm{J \cdot mole^{-1}}$ [18]. Further, the grain boundary thickness or the layer in which diffusion occurs is approximated as $\delta_b = 0.5$ nm [19]. Using these parameters, the diffusion distance during the transient stage, l_s, is of the order of a few nanometers, which is very small compared to a typical grain size of 40 nm. The characteristic time for atoms to diffuse 40 nm is about 2×10^5 s, which is about the same length of time as the plastic strain recovery of the first load-recovery cycle. Thus, grain boundary diffusion likely plays a predominant role in the residual plastic strain recovery. However, the two different characteristic plastic strain recovery rates strongly suggest that there are two different diffusion mechanisms occurring.

Wei et al. [20,21] have attributed the plastic strain recovery process to diffusive processes as well and modeled the process using finite-element analysis by arbitrarily assigning different grain boundaries in the material to have either a high or a low diffusivity. In their model, diffusion is driven by the internal residual stress distribution in the grains introduced by grain boundary sliding during the loading phase of the cycle. In what follows, we present a different model that also assumes plastic strain recovery to be due predominantly to diffusive processes; however, our model is differs substantially different from that of Wei et al. [20,21]. In our model, all grain boundary diffusivities are assumed to be the same and diffusion is driven both by the presence of internal residual stress gradients as well as the presence of nanoscale voids that are known to form during the deformation of NC materials [2,14,22].

We postulate there to be two recovery mechanisms, each of which is dominant in different parts of the recovery phase: in the beginning, diffusion due to highly localized heterogeneous residual stress along the grain boundaries (especially within one grain, since $l_s/l < 1$) causes the relatively high strain recovery rate of $10^{-7}\ \mathrm{s^{-1}}$; while intergrain diffusion and diffusion between grain boundaries and free surfaces are dominant in the steady-state recovery. To demonstrate plausibility, we present a simple model in which the effect of the free surface is taken into account and the constant tensile stress that the film reaches after recovery, also referred as zero-creep stress [23,24], plays an important role.

4. Diffusion-based model of plastic strain recovery

4.1. Overview of diffusion

The geometry of the problem is simplified by assuming two-dimensional grains with grain size, l, as shown in Fig. 5. The chemical potential, which is the increase in free energy of an individual atom added to the system, is denoted as μ, and on the grain boundary is:

$$\mu = \mu_0 - \sigma_n(y)\Omega, \tag{3}$$

where μ_0 is a reference value, Ω is the atomic volume and $\sigma_n(y)$ is the normal stress at the grain boundary (positive for tensile) [25]. In a non-equilibrium state, the gradient of the chemical potential drives atoms along the grain boundary. The atomic flux J_b is given as:

$$J_b = -\frac{\delta_b D_b}{\Omega kT}\frac{\partial \mu_b}{\partial y} = \frac{\delta_b D_b}{kT}\frac{\partial \sigma_n}{\partial y}, \tag{4}$$

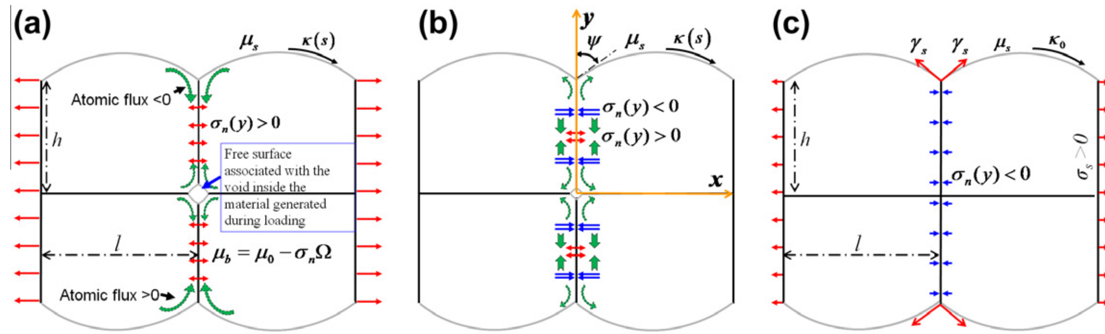

Fig. 5. (a) Schematic of diffusional flux in arrays of 2-D grains under tensile stress. Voids can be generated at joint of multi-grains. (b) Schematic of diffusional flux along grain boundaries and between grain boundary and free surfaces (on voids and film exterior) during plastic strain recovery process after external applied stress removed (c) schematic of final state after plastic strain recovery finishes when zero-creep stress in the film is reached.

where δ_b is the width of the region near the grain boundary through which atoms diffuse, D_b is the grain-boundary diffusivity, k is Boltzmann's constant and T is the absolute temperature [26,27].

These concepts are used to develop a model for recovery of plastic strain based upon concepts pioneered by Darken [28], Herring [29], Hull and Rimmer [30], Chuang and Rice [31], Weertman [32], as well as Needleman and Rice [33], among others. A linear spring model is employed by considering the grain boundary separation $u(y)$ due to the insertion or removal of atoms at the grain boundary. The stress, $\sigma_n(y)$, and grain boundary separation are related as:

$$\frac{u(y)}{l} = -\varepsilon_n = -\frac{\sigma_n}{M}, \tag{5}$$

where M is the plane-strain modulus and ε_n is the average normal strain due to grain boundary separation. Mass conservation along the grain boundary requires:

$$\frac{\partial u(y)}{\partial t} = -\Omega \frac{\partial J_b}{\partial y}. \tag{6}$$

We combine Eqs. (4)–(6), to obtain:

$$\frac{\partial \varepsilon_n}{\partial t} = \frac{\Omega \delta_b D_b M}{lkT} \frac{\partial^2 \varepsilon_n}{\partial y^2}, \tag{7}$$

which is an expression for the strain recovery rate. In what follows, we will employ these concepts to model the plastic strain rate recovery once we have identified possible sources of gradients in chemical potential that will drive the process.

4.2. Mechanisms of plastic strain recovery

We postulate the primary mechanism for plastic strain recovery phenomenon to be that atoms diffuse on grain boundaries from regions of higher chemical potential to regions of lower chemical potential, which ultimately gives rise to the reduction in length of the deformed specimen that is associated with the plastic strain recovery, even in the absence of external loads. The chemical potential gradients are assumed to arise from two different phenomena. In the simple model below, it is demonstrated how the two different chemical potential gradients can lead to two different plastic strain recovery rates.

The first source of chemical potential gradient is due to high gradients of residual elastic strain that develop within the grains of the material as a consequence of grain boundary sliding. Detailed finite-element simulations by Wei et al. [21] of the deformation of NC metals which accounted for the possibility of grain boundary sliding suggested that there can be strong gradients of elastic residual strain established within the grains of the material simply due to the requirements of compatibility of deformation. Thus there are expected to be highly heterogeneous and complex stress gradients within each grain, even after the externally applied loading has been removed. On grain boundaries that connect such grains, the sign of the normal stress on the boundary may oscillate between tension and compression more than once within the length of a typical grain; thus the length scale associated with these stress gradients is expected to be as small as several nanometers. The chemical potential of atoms on the grain boundary is a function of the normal stress as in Eq. (3), so the high stress gradients on the grain boundaries will likely drive diffusion of those atoms relatively rapidly.

The second source of chemical potential gradient is due to the presence of voids that open up in the material as a consequence of the material losing compatibility. Voids can nucleate and grow within NC materials as a consequence of a number of causes, including pre-existing voids on grain boundaries and triple points during film deposition; voids created by dislocations that are nucleated from grain boundaries, as well as voids created due to grain boundary sliding [2,14,22]. Hence, it is natural to expect that a NC thin film that has been plastically deformed as extensively as those of this study will contain a large number of voids both along the grain boundaries as well as at the triple points.

Thus we postulate that the initial plastic strain recovery rate of the order of $10^{-7}\ \mathrm{s}^{-1}$ is due predominantly to the presence of the high residual stress gradients that exist on the grain boundaries. The relatively rapid diffusion serves to "smooth out" the stress gradients themselves. The transition from the initial characteristic plastic strain recovery rate to the slower steady-state rate for plastic strain recovery occurs

due to the lessening of the stress gradients along the grain boundaries as a consequence of grain boundary diffusion.

We postulate the steady-state plastic strain recovery rate to be also due to diffusive flow, but the chemical potential gradient driving the diffusion is due to the difference between that of a free surface and that of a grain boundary, in precisely the same way (but with opposite sign) that diffusion can occur during a sintering process during which powders (often nanometer in size) are able to become consolidated. We assume that this mechanism leads to the majority of the plastic strain recovery in the specimens that occurs at the steady-state plastic strain recovery rate.

Finally, we postulate that the residual tensile stress that exists in the film after plastic strain recovery is introduced as a consequence of diffusive flow between grain boundaries and voids as well as the external surfaces. This is known as the zero-creep stress [24,34,35] which manifests itself as a residual tensile strain on a material that induces a net zero chemical potential gradient throughout a material so that no further deformation via diffusion mechanisms occurs.

4.3. Elements of the model

We refer to Fig. 5 to establish a very simple model for plastic strain recovery. Fig. 5a shows schematically that a free surface can exist either within voids or on an exterior surface. Thus we assume that voids exist in the NC thin film after deformation, likely predominantly at triple points of grain boundaries as shown in Fig. 5a. As suggested in Ref. [36], the diffusion from the voids to the grain boundaries results in a concave void shape.

Fig. 5b establishes the geometry of the model and demonstrates diffusional flux when the external applied stress is removed. The high strain recovery rate is associated with the diffusion along grain boundaries due to the highly localized heterogeneous residual stress; the slow strain recovery is associated with the diffusion between grains and free surfaces. Because the basis of our model is that mass is transferred from the grain boundaries to the voids and the film surface, we must consider the rate at which that mass flux can occur. A kinetic model (e.g. [26]) for the atomic flux at the free surface-grain boundary junction is:

$$J_{gs} = \frac{2C_b\Gamma}{\Omega^{1/3}}\left(1 - e^{-\frac{\Delta\mu}{kT}}\right) \approx \frac{2C_b\Gamma}{\Omega^{1/3}}\frac{\Delta\mu}{kT}, \tag{8}$$

where J_{gs} is the atomic flux from the grain boundary onto a surface (where positive mass flux implies net flow in the y-axis (as defined in Fig. 5b), C_b is the concentration of atoms at the grain boundary and Γ is the jump rate of atoms from the grain boundary to free surface, taking due note that $\Delta\mu/kT \ll 1$. Here we do not differentiate the free surface on the voids from that on the film–air interfaces. The boundary conditions are specified at $y = 0$ and $y = l$ using the pertinent chemical potential difference, $\Delta\mu$, which can be expressed as:

$$\begin{cases} \Delta\mu = [\sigma_s - \sigma_n(y=0,t)]\cdot\Omega & \text{at } y = 0 \\ \Delta\mu = [\sigma_n(y=l,t) - \sigma_s]\cdot\Omega & \text{at } y = l \end{cases}, \tag{9}$$

where σ_s is the steady-state grain boundary stress (also referred as zero-creep stress [23,24]) at which the grain boundary is in equilibrium and $\sigma_n = \sigma_n(y)$ is the normal stress distribution on the grain. From Eqs.3, 7, 8, and 9, the boundary conditions can be written in terms of strain as:

$$\begin{cases} \frac{\partial\varepsilon_n}{\partial y} = \frac{2C_b\Gamma\Omega^{2/3}}{\delta_b D_b}[\varepsilon_s - \varepsilon_n], & \text{at } y = 0 \\ \frac{\partial\varepsilon_n}{\partial y} = \frac{2C_b\Gamma\Omega^{2/3}}{\delta_b D_b}[\varepsilon_n - \varepsilon_s], & \text{at } y = l \end{cases}, \tag{10}$$

where $\varepsilon_s = \sigma_s/M$. Taking $h = l$, the problem can be rewritten by normalizing Eqs. (7) and (10):

$$\frac{\partial\varepsilon_n}{\partial\tilde{t}} = \frac{\partial^2\varepsilon_n}{\partial Y^2}, \tag{11}$$

with boundary conditions

$$\begin{cases} \frac{\partial\varepsilon_n}{\partial Y} = \beta[\varepsilon_s - \varepsilon_n], & \text{at } Y = 0 \\ \frac{\partial\varepsilon_n}{\partial Y} = \beta[\varepsilon_n - \varepsilon_s], & \text{at } Y = 1 \end{cases}, \tag{12}$$

where $Y = y/l$, $\tau = \frac{l^3 kT}{\Omega\delta_b D_b M}$ and $\tilde{t} = t/\tau$. The parameter $\beta = \frac{2C_b\Gamma\Omega^{2/3}l}{\delta_b D_b}$ has physical significance as the degree of strain homogenization along grain boundaries, and is considered a free parameter.

The initial condition for the residual strain, ε_n, immediately after unloading is highly complex and depends upon the details of grain boundary morphology, loading rate, temperature, etc. It is not possible, then, to state the initial conditions of the strain state with any precision. Thus we choose an initial strain distribution that contains the salient elements of the discussion above concerning the diffusion mechanisms. To that end, the following phenomenological expression is used to simulate the heterogeneity of the initial residual strain distribution:

$$\varepsilon_n(Y, t=0) = \varepsilon_1 + \varepsilon_2\cos(\pi Y) + \varepsilon_3\sin(n\pi Y). \tag{13}$$

The first term on the right-hand side of Eq. (13) represents the long-range homogeneous residual strain distribution. The second term represents a long-range heterogeneity in the residual strain distribution that scales with the grain size, l. The third term represents the short-range heterogeneity in the residual strain distribution that corresponds to the short diffusion distance, l_s, in the transient recovery stage, so that $n = l_s/l$. Here, we define $\varepsilon_2 = \alpha_1\varepsilon_{max}$, $\varepsilon_3 = \alpha_2\varepsilon_{max}$ (in which α_1, α_2 are two free coefficients and ε_{max} is the measured initial residual strain immediately after unloading). The value of ε_1 is chosen so that the minimum of $\varepsilon_n(y)$ (residual strain is assigned as negative) is equal to ε_{max}. It should be emphasized that the residual elastic strain distribution is phenomenological and is intended only to capture the salient features of the actual distribution.

4.4. Numerical solution compared to experiments

Given a grain-boundary diffusivity of Cu, $\delta_b D_b$, at $T = 300$ K of 2.03×10^{-30} m^3 s^{-1} according to Ref. [18] and a plane-strain modulus of the Cu films of $M \approx 140$ GPa [5], Eqs. (11)–(13) are solved numerically with free parame-

ters β, α_1 and α_2. Fig. 6a–c shows the comparison of numerical results and experimental data for the first, second and third recovery processes, respectively. For the first recovery, $\beta = 0.4$, $\alpha_1 = 0.22$ and $\alpha_2 = 0.15$ yield the best fit; the second recovery gives $\beta = 0.05$, $\alpha_1 = 0.08$, $\alpha_2 = 0.09$; and the third recovery gives $\beta = 0.05$, $\alpha_1 = 0.10$, $\alpha_2 = 0.16$.

4.5. Zero-creep stress

The steady-state stress, at which diffusion between the grain boundary and free surface stops, is also called "zero-creep stress" [23,34,35]. At equilibrium, the surface chemical potential in the 2-D grain geometry (Fig. 5c) requires a uniform curvature, k_0, which can be expressed as:

$$k_0 = -\frac{2\cos\psi}{l}, \tag{14}$$

where the dihedral angle, ψ, is determined by the balance of local surface tension, i.e. $2\gamma_s \cos\psi = \gamma_{gb}$, where γ_s is the surface energy density and γ_{gb} is the grain boundary energy density. The effective film stress is the combination of normal traction along the grain boundary and in-plane components of the surface tension at the junction, which is expressed as [23,27]:

$$\sigma_s = \frac{1}{h}\int_0^h \sigma(y)dy + \frac{\gamma_s}{h}\sin\psi. \tag{15}$$

The continuity of the chemical potential requires the normal traction at the grain boundary near the junction point, $\sigma(y) = k_0\gamma_s$. Therefore, the steady-state stress, σ_s, can be rewritten as [23,27]:

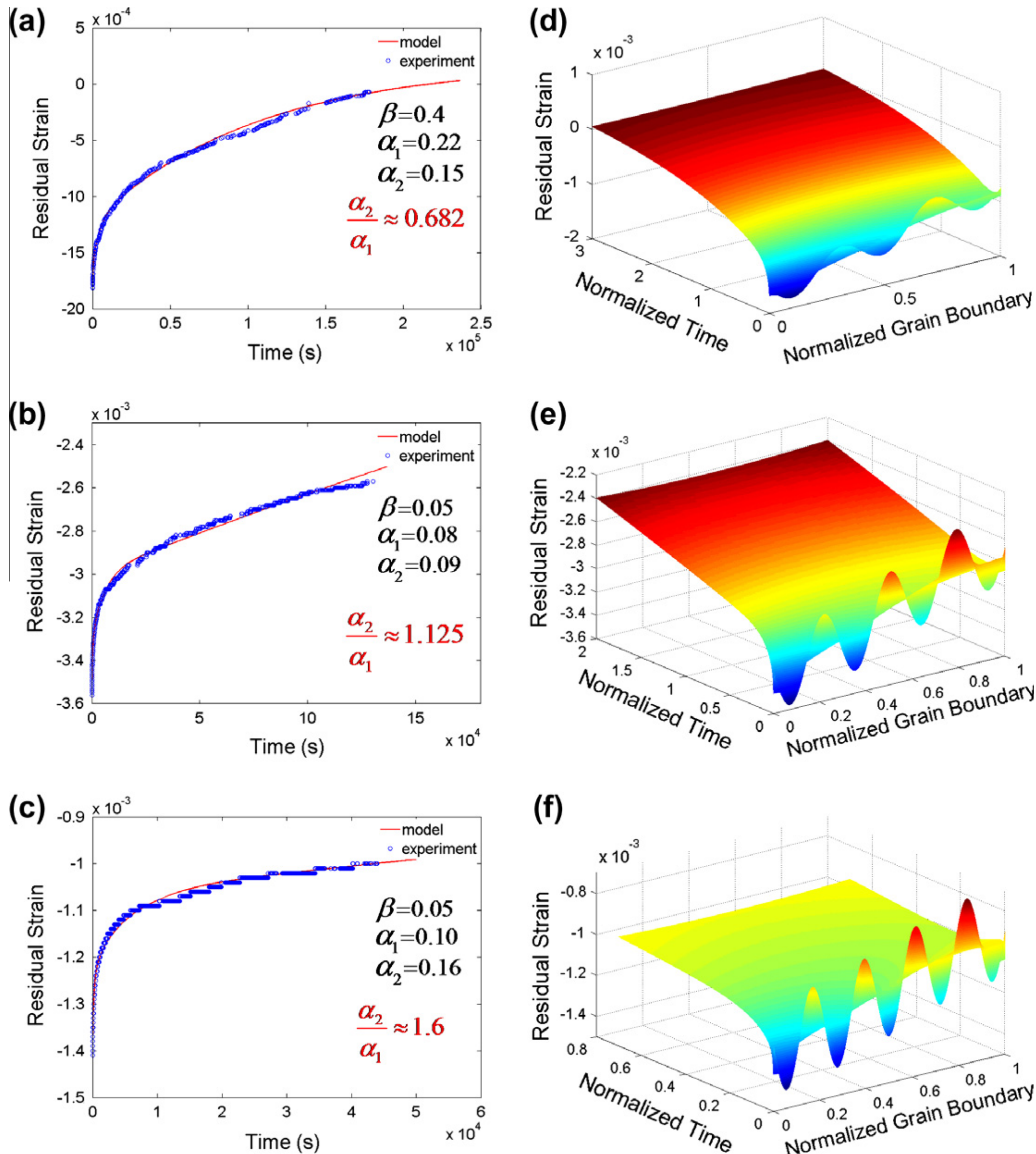

Fig. 6. (a–c) Numerical results and experimental data for the first, second and third recovery processes, respectively. (d–f) Numerical results showing evolution of residual strain along the grain boundary during the first, second and third recovery processes, respectively.

$$\sigma_s = \gamma_s\left(\frac{\sin\psi}{h} - \frac{2\cos\psi}{l}\right). \tag{16}$$

It is clear that the zero-creep stress is mainly sensitive to the geometry of the grains such as grain size and dihedral angle. Taking $h = l = 40$ nm, $\gamma_s \approx 1.52$ J/m^2 [37] and $\psi \approx 80^\circ$, Eq. (16) gives $\sigma_s \approx 24$ MPa, which is consistent with the approximately 25 MPa tensile stress measured after the recovery finishes.

5. Comparison of model to experimental results

The high value of β in the first recovery compared with that in the second and third recovery processes might be due to the much higher tensile initial stress before the first loading (around 170 MPa) since β is expected to be affected by mechanical properties (e.g. surface and grain boundary free energy density, etc.) and the geometry around the junction of the free surface and grain boundary (e.g. dihedral angle, ψ). The second and third recovery processes give a consistent β since the driving force for the recovery is expected to be the stored strain energy during the whole loading/unloading processes, as well as the difference in chemical potential of the grain boundaries and void surfaces. Fig. 6d–f show how the residual strain distributed along the grain boundary evolves for the first, second and third recovery processes, respectively. As discussed before, at the outset of recovery (the transient stage) the short-range heterogeneity of the residual strain is quickly smoothed out due to the very short diffusion distance, l_s. In this stage, the recovery strain rate is up to 10^{-7} s^{-1} for several thousand seconds. However, the steady-state recovery—as postulated—proceeds by continuously driving the atoms out from the grain boundary onto the free surface or voids as controlled by the boundary conditions described in Eq. (12). The steady-state plastic strain recovery rate is of the order 10^{-9} s^{-1}, for a time that can last from several days to about 1 month.

It is interesting that the magnitude of the short-range distributed residual strain is less than that of the long-range distributed residual strain, i.e. the ratio α_1/α_2 is less than unity. However, this ratio consistently increases in the following recovery processes, and α_1/α_2 becomes larger than unity in the third recovery which suggests that the short-range heterogeneity of the residual strain becomes more important with more loading cycles. This suggests that the grain boundaries might change when the film is under loading. For example, grain boundary diffusion and sliding may generate kinks and ledges at the grain boundaries and make the grain boundary geometry more tortuous. Therefore, even after the residual strain is totally recovered, these effects will still remain and affect the process during the next loading cycle.

Finally, it is interesting to compare the experiments from the present study with the experimental results in Ref. [3]. The specimens from both experiments exhibited strain recovery rates of the same order of magnitude. However, the films in the present study recovered the residual strain completely when the loads were removed, while the specimens in Ref. [3] only partially recovered the residual plastic deformation at room temperature. The loading strain rate may contribute to this difference. As Refs. [38,39] suggest, for materials with a similar grain size to that of the specimen used in present study, the dominant deformation mechanisms are grain boundary diffusion and sliding at the strain rate of 10^{-6} s^{-1}, whereas grain boundary diffusion, grain boundary sliding and dislocation activity occur in the materials at the relatively higher loading strain rate of 10^{-4} s^{-1} used in Ref. [3]. The fraction of dislocation activity in the inelastic strain is very difficult to recover as compared with that of the grain boundary diffusion and sliding. Therefore, it is possible that for the specimens in Ref. [3] only the portion of the plastic strain due to grain boundary diffusion and sliding is recovered and the portion due to dislocation activity remains in the material. Thus the extent of plastic strain recovery may depend upon the rate of initial loading.

6. Conclusions

The experiments in this study show that NC Cu films with an average grain size of about 40 nm exhibit a plastic strain recovery phenomenon in that the films recover their residual plastic strain several times after multicycle tests. Two strain rates (transient and steady-state) associated with various diffusion mechanisms are observed during the plastic strain recovery. The film is in a residual state of tension at the end of the plastic strain recovery cycle. Furthermore, partial strain hardening is observed in each subsequent test.

We present a numerical model employing grain boundary diffusion as the predominant recovery mechanism to rationalize this phenomenon. Further, the tensile stress in the film after the plastic strain recovery process is completed can be explained as being the zero-creep stress, which plays an important role in the boundary conditions in our numerical model. The results suggest that grain boundary geometry within the film may change when the film deforms, which, as a feedback, could affect the heterogeneity of the residual strain distribution at the beginning of recovery and also account for the partial strain hardening in the following loading. The results also suggest that the degree of plastic strain recovery achieved during a load–unload cycle may depend upon the strain rate during the loading phase.

Acknowledgments

Support from the Air Force Office of Scientific Research (FA9550-09-1-0048), Lawrence Livermore National Laboratory (B585562) and NSF (DMR-0706058 and CMMI-0826093) is gratefully acknowledged.

References

[1] Kumar K, Van Swygenhoven H, Suresh S. Acta Mater 2003;51(19):5743–74.

[2] Meyers MA, Mishra A, Benson DJ. Prog Mater Sci 2006;51(4):427–556.
[3] Rajagopalan J, Han JH, Saif MTA. Science 2007;315(5820):p–1834.
[4] Hemker KJ. Science 2004;304(5668):221.
[5] Wei X, Lee D, Shim S, Chen X, Kysar JW. Scripta Mater 2007;57(6):541–4.
[6] Chen MW, Ma E, Hemker KJ, Sheng HW, Wang YM, Cheng XM. Science 2003;300(5623):1275–7.
[7] Van Swygenhoven H, Weertman JR. Mater Today 2006;9(5):24–31.
[8] Budrovic Z, Van Swygenhoven H, Derlet PM, Van Petegem S, Schmitt B. Science 2004;304(5668):273–6.
[9] Froseth AG, Derlet PM, Van Swygenhoven H. Adv Eng Mater 2005;7(1–2):16–20.
[10] Siegel RW, Fougere GE. Nanostruct Mater 1995;6(1–4):205–16.
[11] Yamakov V, Wolf D, Phillpot SR, Gleiter H. Acta Mater 2002;50(1):61–73.
[12] Swygenhoven H. Science 2002;296(5565):66.
[13] Wei YJ, Anand L. J Mech Phys Solids 2004;52(11):2587–616.
[14] Wei YJ, Su C, Anand L. Acta Mater 2006;54(12):3177–90.
[15] Ranganathan S, Divakar R, Raghunathan VS. Scripta Mater 2001;44(8-9):1169–74.
[16] Li X, Wei Y, Yang W, Gao H. Proc Natl Acad Sci 2009;106(38):16108.
[17] Tilley R. Principles and applications of chemical defects. Boca Raton, FL: CRC Press; 1998.
[18] Surholt T, Herzig C. Acta Mater 1997;45(9):3817–23.
[19] Wen S, Van D. Ceram Int 1995;21(2):109–12.
[20] Wei YJ, Bower AF, Gao HJ. Scripta Mater 2007;57(10):933–6.
[21] Wei YJ, Bower AF, Gao HJ. J Mech Phys Solids 2008;56(4):1460–83.
[22] Ma Y, Langdon TG. Mater Sci Eng A 1993;168(2):225–30.
[23] Thouless MD. Acta Metall Mater 1993;41(4):1057–64.
[24] Josell D, Weihs TP, Gao H. MRS Bull 2002;27(1):39–44.
[25] Herring C. J Appl Phys 1950;21(5):437–45.
[26] Guduru PR, Chason E, Freund LB. J Mech Phys Solids 2003; 51(11–12):2127–48.
[27] Huang R, Gan DW, Ho PS. J Appl Phys 2005;97(10).
[28] Darken LS. Trans Am Inst Min Metall Eng 1948;175:184–201.
[29] Herring C. Surface tension as a motivation for sintering. In: Kingston WE, editor. The physics of powder metallurgy. New York: McGraw-Hill; 1951.
[30] Hull D, Rimmer DE. Philos Mag 1959;4(42):673–87.
[31] Chuang TJ, Rice JR. Acta Metall 1973;21(12):1625–8.
[32] Weertman J. Scripta Metall 1973;7(10):1129–30.
[33] Needleman A, Rice JR. Acta Metall 1980;28(10):1315–32.
[34] Josell D, Spaepen F. Acta Metall Mater 1993;41(10):3007–15.
[35] Josell D, Spaepen F. Acta Metall Mater 1993;41(10):3017–27.
[36] Tvergaard V. J Mech Phys Solids 1984;32(5):373–93.
[37] Sander D, Ibach H. In: Bonzel H, editor. Physics of covered solid surfaces. Landolt-Börnstein, new series, vol. III-42-A2. Berlin: Springer; 2002.
[38] Wei Y, Bower A, Gao H. Acta Mater 2008;56(8):1741–52.
[39] Wei Y, Gao H. Mater Sci Eng A 2008;478(1–2):16–25.